RESEARCH ARTICLE | MARCH 31 2021

Joint-velocity scalar energy probability density function method for large eddy simulations of compressible flow

Special Collection: In Memory of Edward E. (Ted) O'Brien

Y. Almeida; S. Navarro-Martinez

Physics of Fluids 33, 035155 (2021)
https://doi.org/10.1063/5.0039038

Physics of Fluids ARTICLE scitation.org/journal/phf

Joint-velocity scalar energy probability density function method for large eddy simulations of compressible flow

Cite as: Phys. Fluids 33, 035155 (2021); doi: 10.1063/5.0039038
Submitted: 29 November 2020 · Accepted: 25 February 2021 ·
Published Online: 31 March 2021

Y. Almeida and S. Navarro-Martinez[a)]

AFFILIATIONS

Department of Mechanical Engineering, Imperial College London, London SW7 2AZ, United Kingdom

Note: This paper is part of the special topic, In Memory of Edward E. (Ted) O'Brien.
[a)]Author to whom correspondence should be addressed: s.navarro@imperial.ac.uk

ABSTRACT

The combination of large eddy simulation (LES) and probability density function (PDF) methods is a general framework to model turbulent reactive flows. The coupled approach provides direct closures for the nonlinear subgrid source terms typical of chemically reacting flows. LES-PDF methods have a wide range of applicability and they are started to be used in high-speed flows with strong compressibility effects. However, PDF formulations are more complex in compressible flows, where mechanical and thermodynamic contributions are more coupled. The paper presents a novel PDF framework that uses a full thermodynamic closure (scalar-energy-density-velocity) with the Eulerian Monte Carlo stochastic field approach. The work uses simple closures for the subgrid terms using the advantages of the Eulerian formulation and recasts the stochastic equations in a pseudoconservative form. The resultant formulation is applied to three canonical compressible flows: turbulent shock-tubes, compressible homogeneous turbulence, and a reactive free-moving premixed flame. All cases show large density and pressure fluctuations. The effects of underlying numerical schemes and PDF closures to represent compressible effects are investigated along with the statistical convergence of the method.

I. INTRODUCTION

Probability density function (PDF) methods have been a part of in turbulence modeling since the early 1980s.[1,2] PDF methods provide a framework to incorporate small-scale effects in fluid mechanics simulations. They are particularly advantageous when turbulent small-scale interactions are present, such as in turbulent reactive flows, and scale separation is difficult.

PDF methods have progressed since the pioneering work of the late 1960s and early 1970s[3–5] that formulated the single-point PDF transport equation. PDF approaches started to be applied to turbulent reactive flows,[6,7] when stochastic methods were used to solve the PDF equations. The most common approach was a hybrid Reynolds-averaged Navier–Stokes (RANS)/PDF model where a computational fluid dynamics (CFD) solver would characterize the turbulent flow and a Lagrangian particle solver will be used to represent the PDF evolution. Most of the research development was devoted to characterize the micromixing[8] (or scalar mixing), which represents how small-scale diffusion processes are represented in the PDF equations. All micromixing models suffered limitations under certain conditions (laminar flows, sharp discontinuities, etc.) and the formulation of a general micromixing model is still an unsolved problem. An overview of mixing models is available in Haworth,[8] with model comparison in the works of Subramanian and Pope[9] and Merci *et al.*,[10] among others.

The natural evolution of RANS/PDF methods was the hybrid large eddy simulation (LES) and PDF approach,[11,12] also known as filtered density function, where the PDF is an instantaneous subgrid (or subfilter) distribution. LES removes part of the complexity associated with micromixing, as subgrid PDFs are narrower and simpler models could be used.

The biggest drawback of PDF methods is the cost, and variants have been developed over the years to exploit certain features of the flow to reduce the cost, including conditional moment closure (CMC),[13] multiple mapping condition (MMC),[14,15] direct quadrature method of moments (DQMOM),[16,17] most of which use LES in their recent implementations. However, these methods lose generality or rely on complex closure models. Quoting Piomelli[18] in his 2014 review of LES prospects: "This (LES-PDF) may be, in this author's opinion, one area in which modeling efforts should be focused in the near future."

There are two major stochastic implementations of PDF methods: Lagrangian particles[7] or Eulerian fields.[19,20] In both implementations, the stochastic solvers are often coupled with a more or less conventional CFD solver. The evolution of the stochastic particles and/or fields is discontinuous in time. If a low number of samples is used, due to computational cost, the feedback from the stochastic solver to the CFD has stochastic "noise" that can affect stability. This is particularly important in LES and using Lagrangian methods. Low Mach number solvers (often called incompressible) are usually pressure-based, where the stochastic noise causes oscillations on the continuity constraint. As Mach number increases, compressible effects become important, the momentum and energy equations strongly couple, and explicit density-based solvers become more attractive.

There are two large broad PDF approaches in turbulent reactive flows: joint scalar (hereafter SPDF) and joint velocity-scalar (Langevin-type models[21] or VSPDF). Low-Mach number PDF formulations are relative straightforward (with some exceptions) to derive. However, in compressible flows the formulations are more varied.[22–25]

Lagrangian LES-SPDF applications at high-speed/compressible are limited.[26–28] The main difficulty is to ensure consistency between the scalar/energy scale solved by the PDF and the CFD solver. This involves either smoothing[25] between the particle data transfer or a careful selection of a double transport of energy to ensure consistency.[29] Lagrangian LES-VSPDF[12] approaches are theoretically attractive as they effectively become mesh-less methods. However, their application to compressible flow is still restricted to a few works.[30]

The use of Eulerian stochastic fields to solve a joint SPDF using a compressible formulation was first proposed by Gong *et al.*[31] Similarly, Fredrich *et al.*[32] use a pressure-based compressible method to model thermoacoustic instabilities. In these applications, the sample space did not include an extra thermodynamic variable, such as density or pressure, and compressible effects on the source term were neglected. Other high-speed applications with Eulerian stochastic fields include the work of Pant *et al.*[33] that introduces an improved mixing model. VSPDF applications of stochastic fields in compressible flows are still rare, both in RANS[34] and LES.[35,36]

Despite the recent success, there are still several outstanding issues in LES-PDF of turbulent compressible flows. First, in compressible turbulent flows, advanced numerical methods are required to both capture shock and minimize turbulence dissipation. This is well known in conventional LES,[37] but its effects in LES-PDF are less understood even if numerical diffusion can have a large effect in stability of the method. Moreover, the PDF formulation is not unique, with several approaches reported that expand terms differently or neglect particular contributions (such as subgrid pressure fluctuations). Finally, if LES-PDF are to be successfully and routinely used, convergence with low number of samples must be proved. This paper addresses these points in an Eulerian VSPDF approach with a full closure of the thermodynamic state. The work addresses the effects of numerical schemes and subgrid contributions on the LES-PDF, as well its validation and convergence on several canonical turbulent and high-speed flows.

II. PDF METHODOLOGY

In a system with M degrees of freedom, a fine-grained single-point probability density function is

$$f(\phi_1, \phi_2, \ldots, \phi_M; \mathbf{x}, t) = \prod_{\alpha=1}^{M} \delta(\psi_\alpha(\mathbf{x}, t) - \phi_\alpha), \tag{1}$$

where ϕ_α is the sample variable coordinate associated with the field variable $\psi_\alpha(\mathbf{x}, t)$. In a simple single-phase system with C components, without electrical work, the thermodynamic degrees of freedom are $C+1$ (Gibbs rule) plus 3 due to the components of the velocity: $M = C + 1 + 3$. The selection of the intensive properties that defined the sample space can have a strong influence on the behavior of the model, but *a priori* any choice is valid as long as a closed set is selected. In most LES-PDF applications, only the thermodynamic state is closed and fluctuations in the velocity field are modeled elsewhere (SPDF approaches). In some models, subgrid fluctuations of a particular variable are neglected, in order to improve consistency and/or stability between the CFD and PDF solvers, or because their relative importance is small in the considered system. Neglecting subgrid fluctuations often simplifies the coupling and, hence, the PDF formulation. However, it does not allow a full thermodynamic closure of the source terms or the use of nonideal equations of state. Nik *et al.*[30] first close the thermodynamic state by using specific internal energy and pressure.[26] Unlike RANS-PDF,[22] in LES-PDF does not select turbulence quantities as possible sample variables, although exception exists.[38] In addition to including the reactive scalars, the sample space in LES-PDF may include the specific enthalpy[32] or sensible enthalpy.[27,33]

Following the previous work,[35] the selected variables in this paper are ρ, u_i, e_t (density, velocity, specific total energy) and $(C-1)$ mass-fractions, Y_k. The associated sample space variables are defined by a caret: $\hat{\rho}$, $\hat{u}_i$, $\hat{e}_t$ and $\hat{Y}_k$, and the corresponding sample array is given by $\underline{\phi} = (\hat{\rho}, \hat{u}_i, \hat{e}_t, \hat{Y}_k)$ to be consistent with Eq. (1). Derived quantities are also defined in the same manner: specific internal (chemical and sensible) energy, $\hat{e} = \hat{e}_t - 1/2\hat{u}_i^2$, temperature, $\hat{T} = T(\hat{\rho}, \hat{e}, \hat{Y}_k)$, and pressure, $\hat{p} = p(\hat{\rho}, \hat{e}_i, \hat{Y}_k)$. As mentioned before, this is not the only possible set of variables and the choice depends on the solver and closures. Other variables, such as specific momenta, ρu_i, may be very appealing to formulate the PDF equation.

In a generic formulation, the Navier–Stokes equations can be written as

$$\frac{\partial \psi_\alpha^*}{\partial t} + \frac{\partial u_i \psi_\alpha^*}{\partial x_i} + \frac{\partial J_i^\alpha}{\partial x_i} = S_\alpha(\underline{\psi}), \tag{2}$$

where $\psi_\alpha^* = \rho\psi_\alpha$ (except for density, where $\psi_\rho^* = \rho$,) and J_i^α are the corresponding diffusive flux (stress tensor in the momentum equation) and S_α is the one-point source term, such as chemical reaction or radiation heat flux. Diffusive fluxes in fluid mechanics are generally closed with a gradient-type approach as follows:

$$J_i^\alpha = -D_\alpha \frac{\partial \psi_\alpha}{\partial x_i}, \tag{3}$$

where the diffusion coefficient has an associated molecular scales. In the interest of simplicity, cross-diffusion processes have been neglected, but the above expression can be made general by summing over the thermodynamic space. Similarly, the stress tensor is decomposed into a normal and viscous shear stress τ_{ij}

$$\sigma_{ij} = -p\delta_{ij} + \tau_{ij}. \tag{4}$$

The LES-PDF formalism aims to solve the *probability* of finding a particular state within a filter width Δ at a certain position and

instant $(\mathbf{x}, t)$. The associated single point PDF is obtained by convolution of the fine-grained PDF with a spatial filter G

$$F(\underline{\phi}; \mathbf{x}, t) = \int_\Omega f(\underline{\phi}; \mathbf{x}', t) G(\mathbf{x} - \mathbf{x}'; \Delta) d\mathbf{x}'. \tag{5}$$

The filter function $G(\mathbf{x} - \mathbf{x}'; \Delta)$ is the same used in conventional LES. However, it should satisfy the normalization condition and, for simplicity, it will be considered that the filtering operation commutes with spatial differentiation. The filter should be positive definite and, therefore, $F \geq 0$ everywhere and the probability is well defined.[11] A *filtered* variable is

$$\bar{\psi}(\mathbf{x}, t) = \int_\Omega \psi(\mathbf{x}', t) G(\mathbf{x} - \mathbf{x}'; \Delta) d\mathbf{x}', \tag{6}$$

and a conditionally filtered variables[11,39] is

$$\overline{\langle \psi(\mathbf{x}, t) | \underline{\phi} \rangle} = \int_\Omega \psi(\mathbf{x}', t) f(\underline{\phi}; \mathbf{x}', t) G(\mathbf{x} - \mathbf{x}'; \Delta) d\mathbf{x}'. \tag{7}$$

The hyperbolic nature of the system of Eq. (2) can create discontinuities to form even with smooth initial conditions and make F discontinuous, which contradicts the underlying assumption of single-valued continuous PDF. Nevertheless, the diffusive fluxes will "thicken" the discontinuities, such that the original functions are continuous even if they have a very thin transition, much smaller than Δ. This process is analogous to the vanishing viscosity approach in numerical simulations of the Euler equations.[40] In this work, we assume that, even if shocks can develop, the variables are continuous as $\Delta \to 0$ and, therefore, F is single valued.

The PDF equation can be obtained directly by multiplying (2) by f and using the shift property of PDFs. The resultant expression can be filtered to derived the unclosed LES-PDF equation

$$\frac{\partial F}{\partial t} + \frac{\partial \hat{u}_i F}{\partial x_i} = -\frac{\partial}{\partial \phi_\alpha}\left[\left(S_\alpha(\underline{\phi}) + \overline{\left\langle \frac{\partial J_i^\alpha}{\partial x_i} \middle| \underline{\phi} \right\rangle}\right) F\right], \tag{8}$$

where the source term is closed but the conditional filtered diffusive flux term is unclosed. If the velocity is not included in the selected set (i.e., a SPDF formulation), the convective term will be unclosed $\overline{u_i f}$.

LES-PDF models (and PDF models, in general) diverge on how to approach the closure of the diffusive fluxes and several formulations exist from the same definition of the PDF.[41] As a first approximation, the conditional gradients can be split into a large scale and a subgrid contribution (hereafter, Model I)

$$\overline{\left\langle \frac{\partial J_i^\alpha}{\partial x_i} \middle| \underline{\phi} \right\rangle} = \frac{\partial \bar{J}_i^\alpha}{\partial x_i} + \Psi_{i,sgs}^\alpha, \tag{9}$$

where only the small scales, $\Psi_{i,sgs}^\alpha(\underline{\phi})$ retain the dependence with the sample space $\underline{\phi}$. Alternatively, a Model II splits the conditional gradient into the gradient of the conditional filter and a conditional fluctuation term

$$\overline{\left\langle \frac{\partial J_i^\alpha}{\partial x_i} \middle| \underline{\phi} \right\rangle} = \frac{\partial \overline{\langle J_i^\alpha | \underline{\phi} \rangle}}{\partial x_i} + \Psi_{i,sgs}^\alpha + \Psi''_{i,sgs}, \tag{10}$$

where $\Psi''_{i,sgs}$ is an *ad hoc* term to ensure consistency of the subgird terms between formulations (9) and (10). Subgrid contributions are nearly always modeled in LES-PDF with a drift and diffusion term[42]

$$\Psi_{i,sgs}^\alpha F = A_\alpha(\underline{\phi}) F + \frac{\partial B_{\alpha\beta}(\underline{\phi}) F}{\partial \phi_\beta}. \tag{11}$$

The above functional form is intentional in PDF methods to build a final expression amenable for stochastic treatment. It is clear that the first moment of the subgrid contribution should vanish

$$\int_{-\infty}^{+\infty} \Psi_{i,sgs}^\alpha F(\underline{\phi}) d\underline{\phi} = 0. \tag{12}$$

The drift and the diffusion coefficient (A_α and $B_{\alpha\beta}$, respectively) must preserve the linear properties of subgrid turbulent scalar transport.[43] In the context of conditional moments of passive scalars, the functional form of A and B can be derived. The diffusion term is analogous to the conditional scalar dissipation in conditional moment closure and flamelet type turbulent combustion models.[44] In turbulent mixing, the drift term "narrows" the subgrid PDF reducing fluctuations, while diffusion process "broadens" it. These two terms control the PDF behavior and both contributions require modeling.

The drift term is often represented in LES-PDF as an interaction and exchange with a mean approach[4,45]

$$A_\alpha = \frac{C_\alpha}{\tau_{sgs}}\left(\phi_\alpha - \bar{\psi}_\alpha\right), \tag{13}$$

where τ_{sgs} is a subgrid timescale. In RANS-context, assuming large Reynolds, τ_{sgs} will be proportional to a turbulent timescale. Similarly, the Langevin model,[7,46] can also be written in this form (see Sec. II B). The final general PDF expression (using Model I) would be

$$\frac{\partial F}{\partial t} + \frac{\partial v_i F}{\partial x_i} = -\frac{\partial}{\partial \phi_\alpha}\left[\left(S_\alpha + A_\alpha + \frac{\partial \bar{J}_i^\alpha}{\partial x_i}\right) F\right] - \frac{\partial^2 B_{\alpha\beta} F}{\partial \phi_\alpha \partial \phi_\beta}, \tag{14}$$

which is a Fokker–Planck equation and, therefore, an equivalent stochastic system can be found. The above expression is general and subgrid diffusion terms can be different for each variable. In systems with constant Prandtl/Schmidt numbers, the subgrid turbulent transport is driven by velocity fluctuations only and, therefore, $B_e = B_Y = 0$. In the case of variable Prandtl, these terms would be nonzero and require modeling (following Sec. II B ideas, for example). Similarly in the case of differential diffusion, $B_{jk} \neq 0$, and additional modeling would be needed. No attempt has been done to model these terms in this work and the subgrid fluctuations of the Prandtl and Schmidt numbers are assumed to be small. This assumption is probably moderate in the case of turbulent flows at large Reynolds number or relatively fine meshes.

A. Density weighting

From the PDF derivation point of view, a variable space based on $\psi^* \equiv \rho\psi$ would be preferable, as the convective term would be closed. However, diffusive fluxes are function of gradients of ψ and cannot be easily recast as gradients of ψ^*. Alternatively, a new PDF is defined, the filtered mass density function,[47] $\mathcal{F}$, such that

$$\mathcal{F} \equiv \bar{\rho}\widetilde{f}(\underline{\phi}; \mathbf{x}, t) = \int_\Omega \rho f(\underline{\phi}; \mathbf{x}', t) G(\mathbf{x} - \mathbf{x}'; \Delta) d\mathbf{x}'. \tag{15}$$

The new PDF transport equation will be the same as (8), but with an extra drift term

$$-\frac{\partial}{\partial\phi_\rho}\left[-\bar{\rho}\left\langle\widetilde{\frac{\partial u_i}{\partial x_i}}\middle|\underline{\phi}\right\rangle\mathcal{F}\right]. \tag{16}$$

This is the conditional dilation which, following previous ideas, could be approximated with a Model I approach neglecting subgrid dilation,

$$\bar{\rho}\left\langle\widetilde{\frac{\partial u_i}{\partial x_i}}\middle|\underline{\phi}\right\rangle \approx \bar{\rho}\,\frac{\partial\widetilde{u}_i}{\partial x_i}, \tag{17}$$

or a Model II approach

$$\bar{\rho}\left\langle\widetilde{\frac{\partial u_i}{\partial x_i}}\middle|\underline{\phi}\right\rangle \approx \hat{\rho}\,\frac{\partial\widetilde{\langle u_i|\underline{\phi}\rangle}}{\partial x_i}, \tag{18}$$

that neglects conditional subgrid dilation fluctuations $\bar{\rho}\widetilde{\langle\nabla\cdot u|\underline{\phi}\rangle} - \hat{\rho}\nabla\cdot\widetilde{\langle u|\underline{\phi}\rangle}$. The inclusion of $\hat{\rho}$ (sample variable for ρ) instead of $\bar{\rho}$ indirectly assumes $\hat{\rho}\nabla\cdot\widetilde{\langle u|\underline{\phi}\rangle} \gg \rho''\nabla\cdot\widetilde{u}$. This change will allow later to rewrite the stochastic transport equations in conservative form. Both assumptions do not affect first moments, but this contribution may be important in the immediate vicinity of shocks. In RANS-PDF,[23] dilatation effects were included in the Langevin model (see Sec. II B) or as part of the variable space.[22]

B. Pressure and Langevin term

The conditional stress tensor needs to be modeled

$$\overline{\left\langle\frac{\partial\sigma_{ij}}{\partial x_i}\middle|\underline{\phi}\right\rangle} = \overline{\left\langle\frac{\partial p}{\partial x_i}\middle|\underline{\phi}\right\rangle} + \overline{\left\langle\frac{\partial\tau_{ij}}{\partial x_i}\middle|\underline{\phi}\right\rangle}. \tag{19}$$

The viscous stress contribution will follow a Model I approach, viz.,

$$\overline{\left\langle\frac{\partial\tau_{ij}}{\partial x_i}\middle|\underline{\phi}\right\rangle} = \frac{\partial\bar{\tau}_{ij}}{\partial x_i} + \Psi^{\mu}_{sgs}, \tag{20}$$

where Ψ^{μ}_{sgs} follows a Langevin-type model,[7] with drift coefficient,

$$A_v = G_{ij}(\hat{u}_i - \overline{u_j}), \tag{21}$$

where G_{ij} is the isotropic Langevin tensor defined as

$$G_{ij} = -\frac{1}{\tau_{sgs}}\left(\frac{1}{2}+\frac{3}{4}C_0\right)\delta_{ij} = -\frac{C_1}{\tau_{sgs}}. \tag{22}$$

The associated diffusion coefficient is

$$B_v = \frac{C_0}{2}\epsilon_{sgs}, \tag{23}$$

where ϵ_{sgs} in the subgrid kinetic energy dissipation. Subgrid fluctuations of viscosity have been neglected in this work. To the authors' knowledge, no PDF work has yet attempted to model these fluctuations, but *a priori* it would be possible using Model II-type closures.

In early works on compressible PDF, the pressure effects were included in the Langevin model.[23] In LES-PDF framework,[30] the conditional pressure gradient is often closed using a Model I-approach

$$\overline{\left\langle\frac{\partial p}{\partial x_i}\middle|\underline{\phi}\right\rangle} \approx \frac{\partial\bar{p}}{\partial x_i}, \tag{24}$$

neglecting subgrid fluctuations. Alternatively, in a Model II-type, is possible to split the terms as

$$\overline{\left\langle\frac{\partial p}{\partial x_i}\middle|\underline{\phi}\right\rangle} = \frac{\partial\langle\overline{p|\phi}\rangle}{\partial x_i} + \frac{\partial p''_{sgs}}{\partial x_i}, \tag{25}$$

where p''_{sgs} is the conditional pressure fluctuations. The gradient of the conditional fluctuations may not be negligible and scales with the square of the Mach number. The pressure dilatation term ($u''p''$) in the energy equation can also contribute significantly to subgrid kinetic energy[24] and depending how pressure is approximated, subgrid pressure dilatation may have to be modeled in a similar manner.

C. Stochastic fields

The Favre-filtered PDF can be represented by N_f smooth Eulerian stochastic fields

$$\widetilde{f}(\mathbf{x},t;\underline{\phi}) = \frac{1}{N}\sum_{n=1}^{N_f}\prod_{\alpha=1}^{M}\delta(\phi_\alpha - \xi^n_\alpha(\mathbf{x},t)), \tag{26}$$

where $\xi^n_\alpha(\mathbf{x},t)$ is the stochastic field corresponding to the α-variable, where the associated n-stochastic field variables are: $\varrho^n, \mathcal{U}^n, \underline{\mathcal{Y}}^n, \mathcal{E}^n_t$. A system of stochastic partial differential equations equivalent to the Fokker–Planck can be derived using stochastic characteristic techniques[34] and, in general, form is

$$d\xi^n_\alpha + \mathcal{U}^n_i\frac{\partial\xi^n_\alpha}{\partial x_i}dt = \frac{1}{\bar{\rho}}\frac{\partial\bar{J}^\alpha_i}{\partial x_i}dt + A_\alpha(\bar{\psi}^\alpha - \xi^n_\alpha)dt + B_\alpha dW^n_i + S^\alpha dt, \tag{27}$$

where dW^n_i is a Wiener process with 0 mean and $\sqrt{dt}$ variance and is different from each field. The choice of dilatation model (18) and (25) allows to rewrite the stochastic field equations in conservative form and the final equations are

$$\frac{d\varrho^n}{dt} + \frac{\partial\varrho^n\mathcal{U}^n_i}{\partial x_i} = 0, \tag{28a}$$

$$\frac{d\varrho^n\mathcal{U}^n_i}{dt} + \frac{\partial\varrho^n\mathcal{U}^n_j\mathcal{U}^n_i}{\partial x_j} = -\frac{\partial\mathcal{P}^n}{\partial x_i} - \frac{\partial p_{sgs}}{\partial x_i} + \frac{\varrho^n}{\bar{\rho}}\frac{\partial\widetilde{\tau}_{ij}}{\partial x_i} - \frac{C_1}{\tau_{sgs}}\varrho^n\left(\mathcal{U}^n_j - \widetilde{u}_j\right) + \varrho^n\sqrt{C_0\epsilon_{sgs}}\frac{dW^n_i}{dt}, \tag{28b}$$

$$\frac{d\varrho^n\mathcal{Y}^n_\alpha}{dt} + \frac{\partial\varrho^n\mathcal{U}^n_i\mathcal{Y}^n_\alpha}{\partial x_i} = \frac{\varrho^n}{\bar{\rho}}\frac{\partial\widetilde{J}_{\alpha,i}}{\partial x_i} + \varrho^n S_\alpha(\underline{\mathcal{Y}}^n, \mathcal{T}^n, \mathcal{P}^n) - \frac{C_Y}{\tau_{sgs}}\varrho^n\left(\mathcal{Y}^n_\alpha - \widetilde{Y}_\alpha\right), \tag{28c}$$

$$\frac{d\varrho^n\mathcal{E}^n_t}{dt} + \frac{\partial\varrho^n\mathcal{U}^n_i\mathcal{H}^n_t}{\partial x_i} = \frac{\varrho^n}{\bar{\rho}}\frac{\partial\widetilde{q}_i}{\partial x_i} + \frac{\varrho^n}{\bar{\rho}}\frac{\partial\widetilde{\tau}_{ij}\widetilde{u}_j}{\partial x_i} - \frac{C_e}{\tau_{sgs}}\varrho^n\left(\mathcal{E}^n_t - \widetilde{e}_t\right), \tag{28d}$$

where $\mathcal{H}_t = \mathcal{E}_t + \mathcal{P}/\varrho$ is the stochastic field total enthalpy. The final equations ensure that each stochastic field conserves mass and has a consistent thermodynamic state. Viscous and molecular transport terms have been modeled using Model I, where a $\varrho^n/\bar{\rho}$ contribution appears. The continuity and momentum equations resemble the expressions proposed by Azarnykh *et al.*[48] The set of Eqs. (28) can be

readily implemented in a density-based explicit code. Using conventional compressible formulation,[40] where U is the array of conservative variables, the implemented equations are

$$\frac{dU^n}{dt} + \nabla F(U^n) = \frac{\varrho^n}{\bar{\rho}} \nabla F_{vis}(\bar{U}) + S^n(U^n) + A^n_{sgs}(U^n, \widetilde{U}) + B^n_{sgs} \frac{dW^n}{dt}, \tag{29}$$

where $F(U)$ is the Euler fluxes and F_{vis} is the viscous fluxes. The terms A_{sgs} and B_{sgs} represent the generic drift and stochastic contributions, respectively, with $\sum_n A^n_{sgs}/N_f = 0$. The conservative form ensures that the stochastic fields are well behaved, albeit this is not a necessary condition. If the pressure is represented using a Model I (24), the Euler fluxes use the mean pressure $\bar{p}$, while in Model II the stochastic pressure $\mathcal{P}^n$ is used instead. In Model II, the thermodynamic state is completely closed, the pressure and temperature of the stochastic fields can be directly obtained from stochastic variables using the relevant equations of state $\mathcal{P}^n = p(\varrho^n, \mathcal{U}^n_i, \mathcal{E}^n_t, \underline{\mathcal{Y}}^n)$ and $\mathcal{T}^n = T(\varrho^n, \mathcal{U}^n_i, \mathcal{E}^n_t, \underline{\mathcal{Y}}^n)$. Nonideal equations of state, temperature dependence of the specific heats and generic nonideal behavior are directly closed, without the need of further models. The formulation (29) will be stable if the stochastic field acoustic Courant–Friedrichs–Lewy (CFL) number (based on the field velocity and speed of sound) is less than unity. Physical boundary conditions are the same as $\bar{U}$ and subgrid turbulent inflow conditions can be easily implemented. Nonreflective boundary conditions[49] could be applied to each field separately, although it has not been implemented in this work.

1. Subgrid modeling

To maintain consistency between the different LES closures, the subgrid frequency timescale, is defined as the ratio between subgrid kinetic energy and its dissipation

$$\frac{1}{\tau_{sgs}} = \frac{k_{sgs}}{\epsilon_{sgs}}. \tag{30}$$

Assuming local equilibrium between turbulent production and dissipation at subgrid scales, ϵ_{sgs} is modeled as

$$\epsilon_{sgs} = C_\epsilon k^{3/2}_{sgs}/\Delta, \tag{31}$$

where $C_\epsilon = 1.05$ and the micromixing constants C_Y and C_e are set to 2 and the Langevin constant $C_0 = 2.1$, following LES-PDF convention.[50] The subgrid specific kinetic energy, k_{sgs}, can be directly obtained from the stochastic fields information

$$k_{sgs} = \frac{1}{2} \frac{1}{N_f} \sum_{n=1}^{N_f} (\mathcal{U}^n_i - \widetilde{u}_i)^2. \tag{32}$$

The VSPDF formulation does not need any Smagorinsky-type closures typical in LES, such as $\tau_{sgs} \propto ||\bar{S}_{ij}||^{-1}$, and only the model (31) is required.

The filtered variables can be obtained from the average of the Eulerian stochastic fields. For a variable $\psi(\mathbf{x}, t)$, it is possible to recover the filtered and the Favre-filtered values form the associated field $\xi^n_\alpha(\mathbf{x}, t)$ by

$$\bar{\psi}_\alpha = \frac{1}{N_f} \sum_{n=1}^{N_f} \phi^n_\alpha \quad \widetilde{\psi} = \frac{\sum_{n=1}^{N_f} \varrho^n \phi^n_\alpha}{\sum_{n=1}^{N_f} \varrho^n}. \tag{33}$$

The stochastic equations (28) have been implemented in the finite difference solver CompReal.[35,51] The main numerical scheme used is the fourth-order dispersion-relation-preserving (DRP) scheme.[52] The DRP scheme is a high-order, low-dispersive, and low-dissipative explicit scheme.[53] The convective terms are discretized through a hybrid DRP/HLLC-TVD scheme, where the Harten-Lax-van Leer-Contact (HLLC) Riemann solver[54] is used to discretize the Euler fluxes close to discontinuities with a second order total variation diminishing (TVD) reconstruction. The coupling is performed using a sensor similar to the one of Martinez Ferrer *et al.*[55] using the pressure jump between neighboring cells as discriminant. The remaining spatial derivatives are discretized with a fourth-order classical central differences. The resultant scheme is formally second-order close to discontinuities and fourth away from them.

III. RESULTS

A. Subgrid pressure: Riemann problem

The use of a Model-I type of closure makes the system unstable in supersonic turbulent flows,[35] as the Euler fluxes are not self-consistent. Guillois *et al.*[56] proposed a similar Model I closure for an Eulerian Monte Carlo VPDF, which was stable in compressible flows, using a Random Choice Method[57] transport scheme.

To illustrate the effects of subgrid pressure, the one-dimensional turbulent Riemann problem from Soulard and Sabelnikov[20] is chosen, which is a modification of classic Sod's test case.[40] The domain is initially divided into a left and right state with 0-mean velocity

$$\text{left state } (x < 0.5\,\text{m}) \begin{cases} \widetilde{u''^2} = 50\,\text{m}^2/\text{s}^2 \\ \bar{\rho} = 0.729\,\text{kg/m}^3 \\ \bar{p} = 10^5\,\text{Pa} \end{cases}$$
$$\text{right state } (x < 0.5\,\text{m}) \begin{cases} \widetilde{u''^2} = 0\,\text{m}^2/\text{s}^2 \\ \bar{\rho} = 0.456\,\text{kg/m}^3 \\ \bar{p} = 5 \times 10^4\,\text{Pa} \end{cases}. \tag{34}$$

The velocity distribution is chosen to reproduce a Gaussian distribution. For simplicity, a constant subgrid frequency of $1/\tau_{sgs} = 200\,\text{s}^{-1}$ is used to be consistent with the original test.[20] Zero-gradient boundary conditions were selected with a uniform mesh of $N_x = 320$ grid points. Simulations with $N_f = 16$ and 128 fields were employed. A pure HLLC-TVD scheme is used and, under these conditions, Model I is stable.

Figure 1 shows the evolution of the velocity with $N_f = 16$. The results of Model I are qualitatively and quantitatively very similar to the results reported by Soulard and Sabelnikov.[20] Velocity fluctuations are not transported with the generated shock wave characteristics but with the filtered flow field, $\bar{u}$, and do not cross the contact wave (at $x = 0.55$ m). However, using Model II, each stochastic field has their own pressure, the stochastic fields uncoupled and velocity fluctuations follow separate shock characteristics, propagating at acoustic speeds,

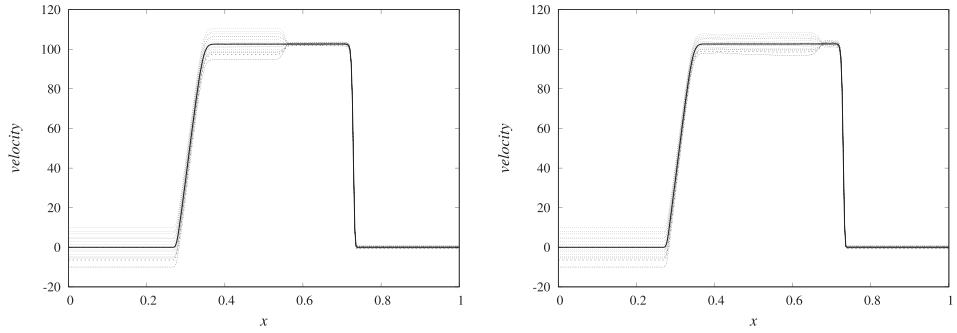

FIG. 1. Velocity field at $t = 5 \times 10^{-4}$ s, solid line indicates mean $\widetilde{u}$, while lighter line indicates the stochastic velocity field. (Left) Model I. (Right) Model II with $\nabla p_{sgs} = 0$.

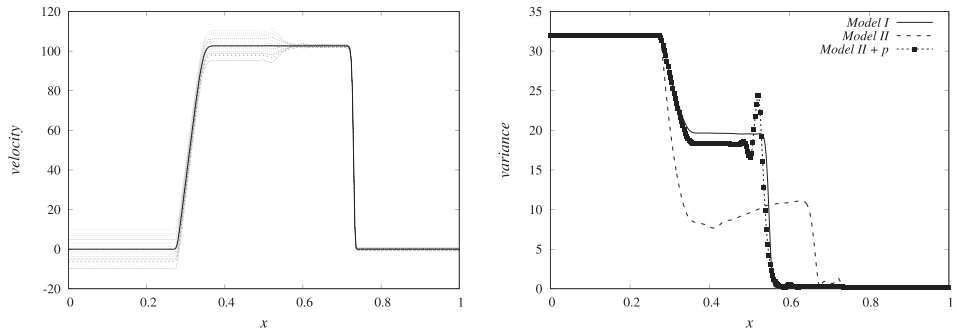

FIG. 2. Velocity distribution at $t = 5 \times 10^{-4}$ s, solid line indicates mean $\widetilde{u}$, while lighter line indicates individual stochastic velocity field. (Left) Mean velocity, $\widetilde{u}$. (Right) Velocity variance, $\widetilde{u''^2}$.

which is unrealistic. Moreover, the velocity variance is markedly smaller within the moving wave (see Fig. 2 right). A similar effect was previously reported in an early work.[35] Nevertheless, the mean shock structure is very similar in both cases and close to the exact solution as velocity fluctuations are moderate.

Following Model II framework, in the stochastic field formulation, the subgrid pressure fluctuation can be estimated by $p_{sgs} = \bar{p} - \mathcal{P}^n$ and a term ∇p_{sgs} is added to the momentum equations using central differences. The term adds a drift contribution that acts as a subgrid force to reduce velocity. The results show that the velocity follows the expected behavior (see Fig. 2). Subgrid velocity variance also has similar levels to Model I and the variance increases close to the contact wave.

There is no analytical solution to this problem, as subgrid fluctuations exist independent of the mesh, and it is not clear which is the correct turbulence level. Using a mean pressure gradient, Model I uncouples the velocity fluctuation for the other variables quantities, as all fields see the same pressure-dilatation, and associated temperature fluctuations are very small (less than 0.02% compared to approximately 7% in velocity). The coupling is retained in Model II, and larger temperature fluctuations are predicted. It is worth noting that, with the specified initial conditions (34), the initial total energy has subgrid fluctuations (see Fig. 3).

B. Numerical methods: Homogeneous isotropic turbulence

The HLLC-TVD scheme used in Sec. III A is not suitable for LES as the excessive numerical diffusion will quickly dissipate turbulence. To showcase the ability of the numerical schemes to recover the theoretical kinetic energy spectra, a compressible homogeneous isotropic turbulence cube configuration[58] is used with a random velocity field with an imposed spectra $E(k)\,k^4 e^{-2(k^2/k_0^2)}$, with $k_0 = 2$. The initial pressure field is obtained by solving a Poisson equation assuming incompressibility. The initial density field is then set equal to unity

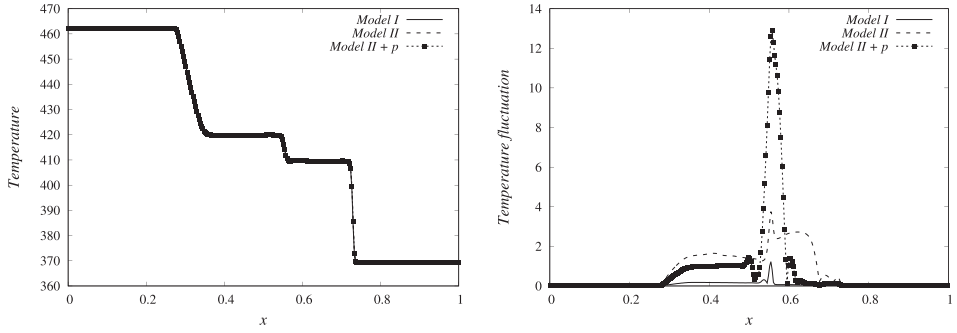

FIG. 3. Temperature distribution at $t = 5 \times 10^{-4}$ s. (Left) $\widetilde{T}$. (Right) Subgrid fluctuation $\sqrt{\widetilde{T''^2}}$.

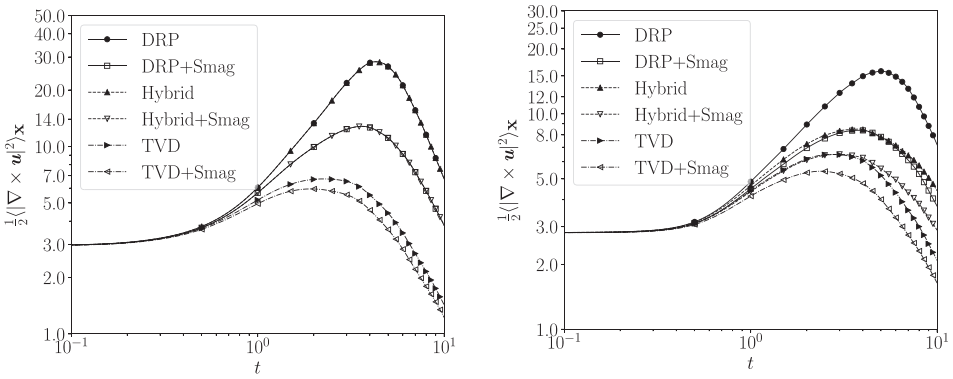

FIG. 4. Spatial averaged enstrophy temporal evolution: (left) $\mathrm{Ma}_{rms} = 0.2$; (right) $\mathrm{Ma}_{rms} = 1$.

and the temperature is then obtained from the ideal gas equation of state

$$\frac{\rho}{p} = \frac{T}{\gamma \mathrm{Ma}_{rms}}, \tag{35}$$

with $\gamma = 1.4$. Two cases were selected, the first with turbulent Mach number, $\mathrm{Ma}_{rms} = 0.2$ which represents a low compressibility case, and the second with $\mathrm{Ma}_{rms} = 1.0$ (high compressibility). The domain is a periodic cube with length 2π discretized with 64 elements in all directions where all boundary conditions are periodic. The simulations were carried up to $t = 10$, in order to allow $10/\pi \approx 3$ initial eddy-turnover times.[58]

Figure 4 compares the enstrophy evolution of different numerical schemes applied in a conventional LES configuration with a Smagorinsky model. The position of the peak is a measure of the numerical diffusion of the scheme and earlier peaks will suggest more diffusive schemes.[59]

For the low Mach number case, the difference between the hybrid and the DRP scheme is negligible since there are no sharp gradients generated and the hybrid scheme converges to the DRP discretization. All spectrum obtained with the Smagorinsky model follow the $-5/3$ decay, although the TVD model dissipates the energy significantly faster. All DRP-based schemes showcase the high wave-number dissipation due to an explicit 13 point stencil filter. At the more compressible case, $\mathrm{Ma}_{rms} = 1$, shocks develop, and the hybrid scheme dissipates more energy than the pure DRP scheme. Numerical viscosity added by the TVD scheme and dissipation by the Smagorinsky model damp the peak magnitude and shift the peak to an early time.

Although the DRP schemes are the most accurate, their instability when combined with stochastic equations prevent their use unless in a hybrid context. Figure 5 shows the enstrophy evolution with different schemes using LES/Smagorinsky and the current LES-VSPDF approach. The DRP, combined with VSPDF, promotes unrealistic early enstrophy growth, followed by a sudden decay. The hybrid-VSPDF maintains a stable solution, with little dissipation and its use is a good compromise for stochastic field simulations. At $t > 8$, the hybrid + VSPDF model destroys enstrophy quicker than the pure hybrid solution and the approach behaves like the Smagorinsky model at $t = 10$. At $t = 10$, the flow is quasi-incompressible, with small density fluctuations, and LES models with the same resolution and numerical approach will behave similarly.

Another important tool to evaluate the flow development is the analysis of the maximum and minimum density ratio within the domain.[59] Figure 6 shows how the Smagorinsky model reduces the density ratio. At $t \approx 3.5$, the Smagorinsky model prevents the appearance of a shock and the growth of maximum density. Overall, VSPDF manages to maintain the density fluctuations without additional dissipation.

C. Stochastic convergence: Reactive shock tube

To assess the statistical performance of the LES-PDF model, a one-dimensional reactive shock tube is used with detailed chemistry mechanism. The test case, originally proposed by Fedkiw *et al.*,[60] is a

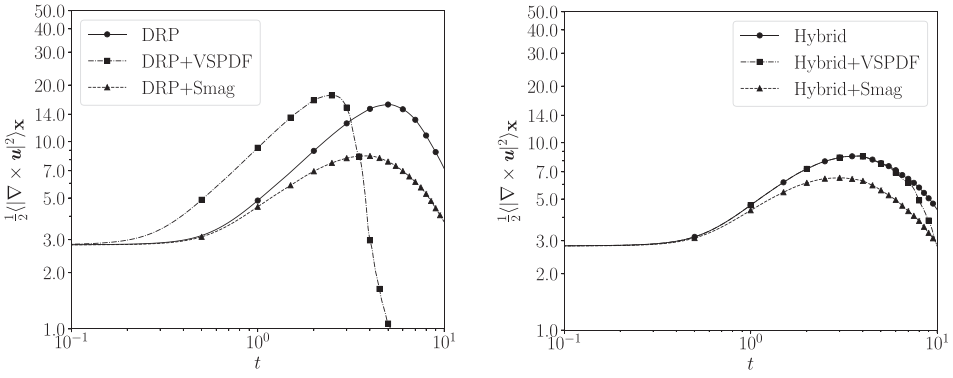

FIG. 5. Spatial averaged enstrophy temporal evolution. (Left) DRP-schemes. (Right) Hybrid-schemes.

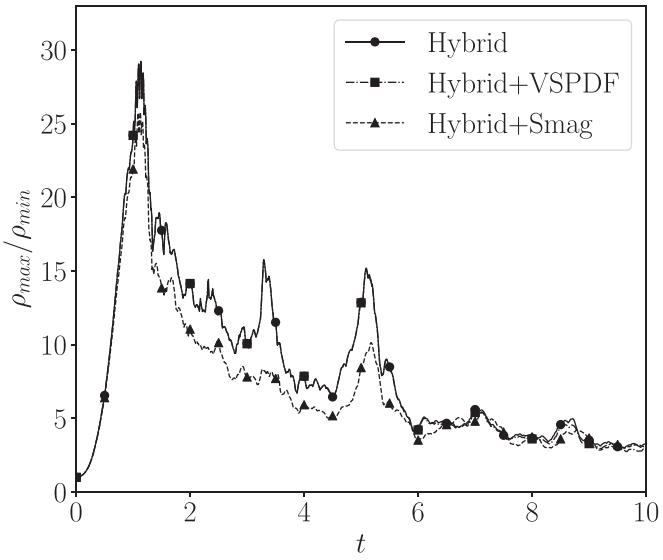

FIG. 6. Density ratio evolution with time $\mathrm{Ma}_{rms} = 1$.

one-dimensional reactive shock tube with initial mole fraction ratio of 2/1/7 for $H_2/O_2/Ar$ in the whole domain. A 9 species and 18 reactions hydrogen combustion detailed mechanism[61] is employed. The shock tube has a length 0.12 m and the following initial conditions:

$$\begin{aligned}
&\text{left state } (x < 0.06\,\text{m}) \begin{cases} \bar{\rho} = 0.072\,\text{kg/m}^3 \\ \widetilde{u} = 0\,\text{m/s} \\ \bar{p} = 7173\,\text{Pa} \end{cases} \\
&\text{right state } (x > 0.06\,\text{m}) \begin{cases} \bar{\rho} = 0.18075\,\text{kg/m}^3 \\ \widetilde{u} = -487.34\,\text{m/s} \\ \bar{p} = 35594\,\text{Pa}. \end{cases}
\end{aligned} \tag{36}$$

The initial Mach number is 0.89, while the left boundary is a wall and zero gradient is applied to the boundary condition at the right. The hybrid DRP/TVD spatial discretization is employed in all test cases for the convective term, while the remaining spatial derivatives are discretized using fourth-order finite differences. Temporal integration is performed using an explicit third-order Runge–Kutta scheme. The pressure wave will travel to the left, hit the wall, and increase pressure and temperature igniting the mixture, generating a deflagration wave toward the right. The mesh convergence was evaluated from 50 to 6400 nodes, with a simulation with $N_x = 6400$ without any model considered a 1D-DNS (direct numerial simulation) solution with $\Delta \approx 19\mu$m. This is not strictly a "turbulence" DNS, but a simulation where all fluid and molecular transport scales are resolved. Turbulence does not a play a role in this simulation but subgrid scales do. Simulations with $N_x = 400$ ($\Delta \approx 300\mu$m), were consider quasiconverged and the number of fields was changed from $N_f = 2$ to $N_f = 8192$. The solution with 8192 fields is considered the reference solution to evaluate the convergence for the PDF model.

The results are compared with a conventional LES joint scalar PDF[35] (hereafter, SPDF) and a conventional Smagorinsky closure without subgrid combustion model, with the same discretization schemes. Figure 7 shows that the VSPDF results are the closest to the DNS data. The SPDF model generates excessive diffusion, which accelerates the flame. Similarly, the Smagorinsky approach, without subgrid combustion model, also slightly accelerates faster than DNS.

Introducing the LES-PDF correction proposed by Jones *et al.*[62] on the τ_{sgs} (a somehow similar correction was proposed by Valiño *et al.*[63]) ensures that $\tau_{sgs} \to 0$ in laminar flows, and the results of the SPDF are very close to the VSPDF solution (see Fig. 8).

Centered moments are used to investigate the convergence of the statistical moments. The ith centered moment (for each component of the sample space) is

$$\mu_i = \int_{-\infty}^{+\infty} (\phi - \mu_1)^i F(\phi; x, t) d\phi, \tag{37}$$

and from the stochastic fields

$$\mu_i^{N_f} = \frac{1}{N_f} \sum_{n=1}^{N_f} \left(\xi^n - \mu_1^{N_f} \right)^i. \tag{38}$$

The convergence error is defined by normalizing the error respect the corresponding moment with $N_f = 8192$. The first two moments show a very good instantaneous convergence (see Fig. 9) at a fix point,[64] with first moment even achieving higher than the expected $N^{-1/2}$ in velocity, fuel, and products. The instantaneous errors are relatively large as the flame slightly moves as the number of fields increase. Similar convergence behavior (not shown) is observed in the SPDF model. The flame position is where scalar, velocity and pressure gradients are stronger. The statistically convergence is therefore likely to be the same in the smooth parts of the flow. Higher moments, however, seem to have lower convergence rates, with 3rd and 5th moments having a slower convergence rate of 0.2–0.4 rather than the expected 0.5. Convergence of high statistical moments may also depend on the implementation of the Wiener term.[65]

The results for the spatially averaged relative error are shown in Fig. 10 for the first six moments. Convergence rates 0.3–0.5 are obtained for nearly all moments. Errors lower than 5% can be obtained on the mean with $N_f = 10$. However, a much larger number of fields is required if the same error is expected in higher moments ($N_f > 100$). Even if instantaneous convergence of the solution seems slow, in practical simulations results are averaged over a large number of steps and time-averaged statistical errors would be much smaller.

The VSPDF model scatter of fields at the flame front produces relatively small fluctuations of 300 K in one cell, with a strong correlation between temperature and water concentration (see Fig. 11).

The quasi-Gaussian subgrid behavior of the fields is observed in Fig. 12, where the subgrid PDF is compared with a Gaussian fit. This combined with the relatively good agreement of all the models at the present resolution, suggest that subgrid behavior may not be than important, and $\overline{S(Y)} \approx S(\bar{Y})$. The flame is close to detonate and gas-dynamics dominate over diffusion process. Under these conditions, high-resolution and reaction-driven flame dynamics, simpler LES approaches may be more cost-efficient.

IV. CONCLUSIONS

The paper assesses a novel Eulerian Monte Carlo joint velocity-scalar-energy PDF formulation. The proposed methodology is very

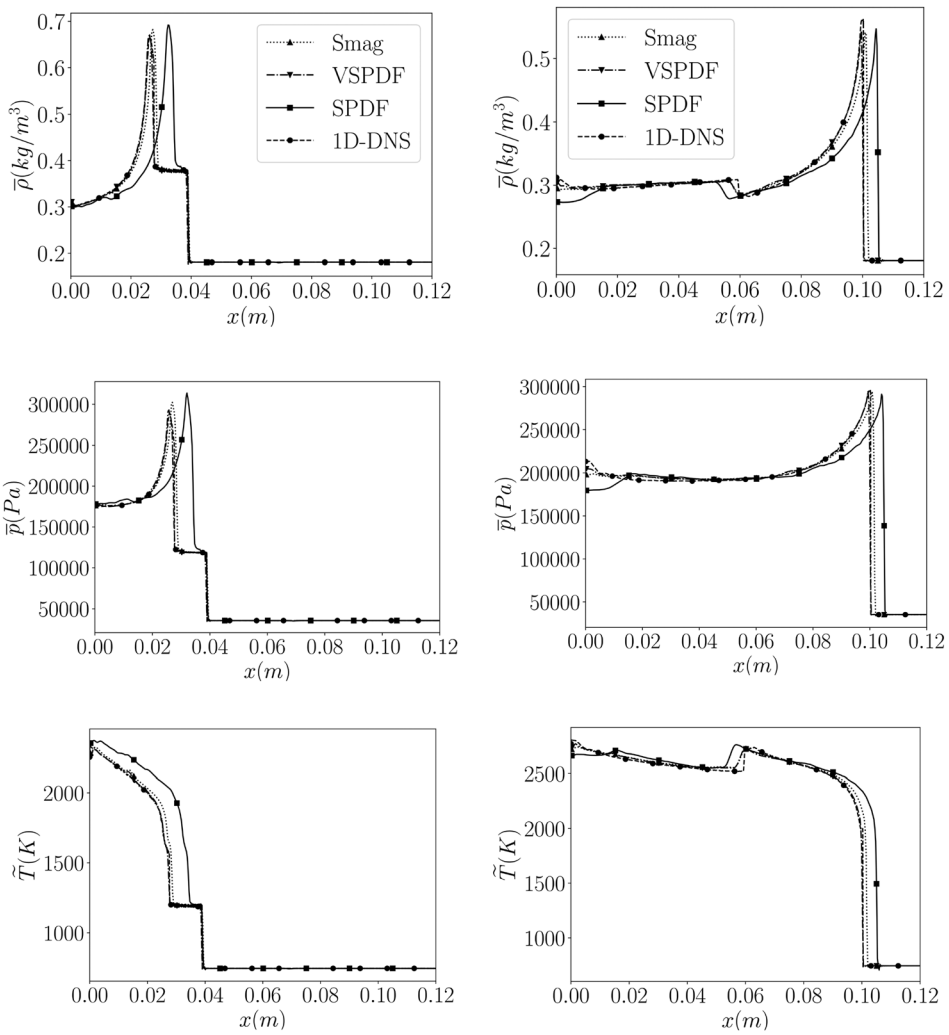

FIG. 7. Results for reactive shock tube at $t = 160\ \mu s$ (left) and $t = 230\ \mu s$ (right).

general and the thermodynamic state is completely closed, where each field has their own self-consistent thermodynamic state and, therefore, subgrid pressure effects, and nonideal gases effects are naturally included without additional modifications. Effects of *subgrid* fluctuations of the transport coefficients (viscosity, diffusivity, etc.) have not been included (nor subgrid fluctuations of Prandtl or subgrid differential diffusion effects), but could, in principle, be addressed in a similar manner as subgrid pressure and dilation effects. Re-casting the stochastic field equation in conservative form increases the stability of the system as well as the ease of implementation in CFD codes.

Neglecting conditional subgrid pressure fluctuations leads to uncoupling of the stochastic momentum equations and a reduction of

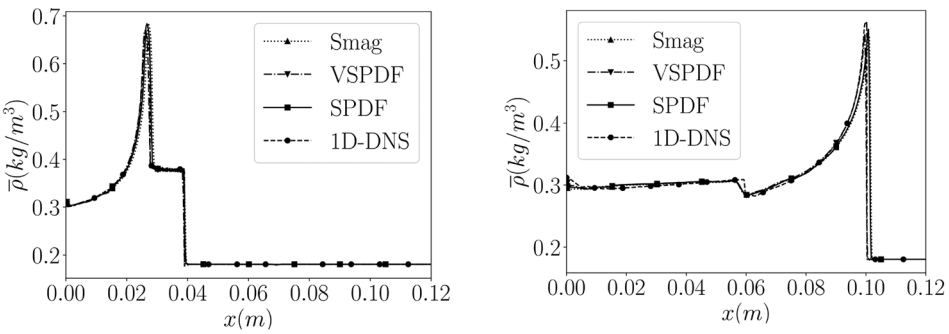

FIG. 8. Results for reactive shock tube at $t = 160\ \mu s$ where the SPDF model includes the τ_{sgs} correction.

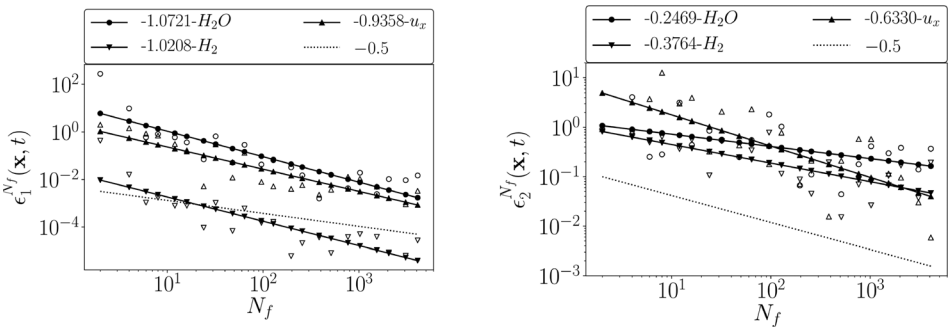

FIG. 9. Instantaneous convergence error (normalized) at approximately the flame position at $t = 230\ \mu$s. The solid line indicates best fit and the numbers the slope.

the velocity variance with erroneous turbulence propagation. Neglecting completely subgrid pressure fluctuations recovers the correct behavior but destroys the pressure dilation ability to generate fluctuations. The inclusion of a subgrid pressure gradient through a simple drift approach allows to recover the right fluctuation levels.

The selected hybrid finite-difference/TVD model with VSPDF maintains turbulence levels and the behavior in a compressible homogeneous isotropic, outperforming the Smagorinsky model. The numerical diffusion due the shock capturing negatively affects the model similarly to other high-speed compressible LES. A possible

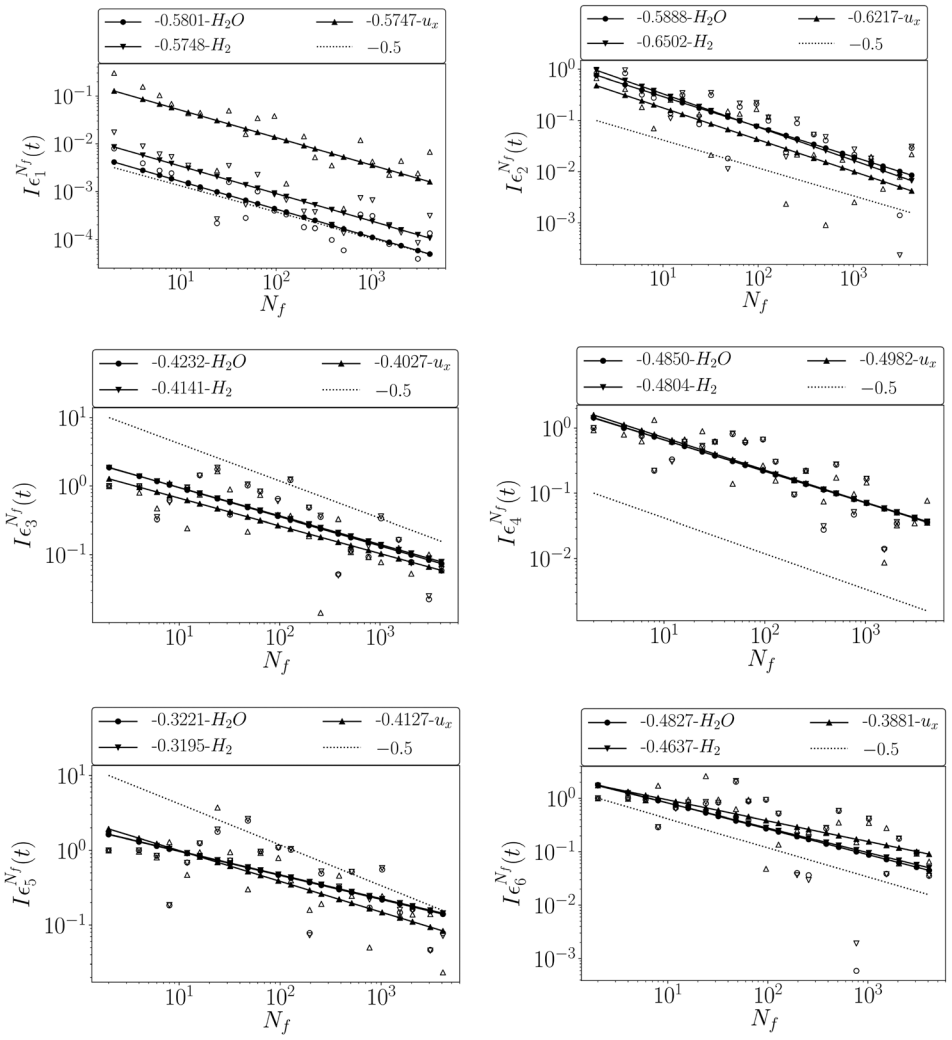

FIG. 10. Instantaneous spatially averaged convergence error (normalized) at approximately the flame position at $t = 230\ \mu$s. The solid line indicates best fit and the numbers the slope.

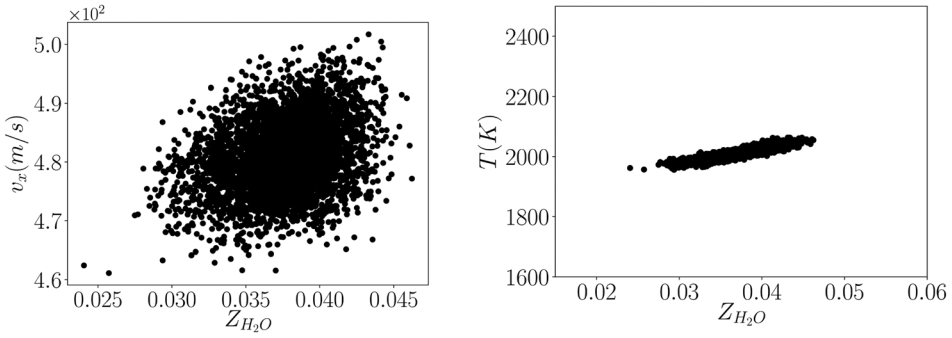

FIG. 11. Instantaneous scatter plots at the flame front position $x = 0.1$ m for the velocity (left) and temperature (right) at $t = 230\ \mu$s.

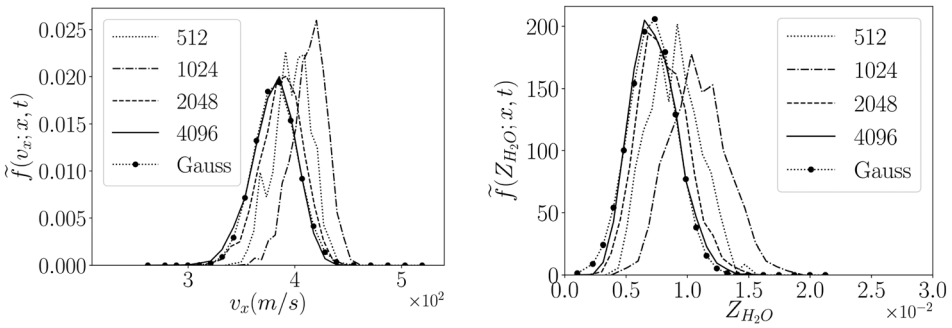

FIG. 12. Marginal PDF distribution at the flame front position $x = 0.1$ m for the velocity (left) and temperature (right) at $t = 230\ \mu$s. The solid lines indicate solutions with different N_f.

improvement will be the use of anisotropic Langevin models[46] and reduce the subgrid turbulence dissipation rate close to discontinuities; where turbulence models and numerical diffusion co-exist. Similarly, the choice of subgrid timescale constants may have to be revisited under these conditions.

The cost of the method is directly proportional to the number of fields used. A simulation with $N_f = 1$ would have a similar cost as LES without any subgrid model. The method shows close to theoretical statistical convergence and the first moment converge with relatively low number of fields $N_f \approx 10$. However, many more fields may be needed if instantaneous convergence of higher statistical moments is required. If this is the case, dedicated acceleration techniques such as adaptive mesh refinement of the stochastic fields will have to be employed. Similarly, if the grid is fine enough that velocity and scalar subgrid fluctuations are small, cheaper LES models may be more cost-effective. However, this may be difficult to know *a priori*. Overall, the new LES-VSPDF method is able to reproduce compressible canonical turbulent and shock flows. If a stable high-order low-dispersion CFD solver is available, the framework allows to quickly create a LES model to account for joint subgrid fluctuations of any thermodynamic-velocity state. This is particularly desirable for modeling compressible reacting flows, such as high-speed combustion, detonations, and hypersonic reentry flows.

ACKNOWLEDGMENTS

Y. Almeida acknowledges the financial support provided by the Brazilian National Council for Scientific and technological Development (CNPq) through the Science without Borders programme, Grant No. 233815/2014–7.

DATA AVAILABILITY

Data were generated at Imperial College London. Derived data supporting the findings of this study are available from the corresponding author upon request.

REFERENCES

[1]E. E. O'Brien, "The probability density function (pdf) approach to reacting turbulent flows," in *Turbulent Reacting Flows*, edited by P. A. Libby and F. A. Williams (Springer Berlin Heidelberg, Berlin, Heidelberg, 1980), pp. 185–218.
[2]S. B. Pope, "A Monte Carlo method for the PDF equations of turbulent reactive flow," Combust. Sci. Technol. **25**, 159–174 (1981).
[3]T. S. Lundgren, "Distribution functions in the statistical theory of turbulence," Phys. Fluids **10**, 969–975 (1967).
[4]C. Dopazo, "Probability density function approach for a turbulent axisymmetric heated jet. Centerline evolution," Phys. Fluids **18**, 397–404 (1975).
[5]S. B. Pope, "The probability approach to the modelling of turbulent reacting flows," Combust. Flame **27**, 299–312 (1976).
[6]J. Janicka, W. Kolbe, and W. Kollmann, "The solution of a PDF-transport equation for turbulent diffusion flames," in Proceedings of the 1978 Heat Transfer and Fluid Mechanics Institute (1978).
[7]S. B. Pope, "PDF methods for turbulent reactive flows," Prog. Energy Combust. Sci. **11**, 119–192 (1985).
[8]D. C. Haworth, "Progress in probability density function methods for turbulent reacting flows," Prog. Energy Combust. Sci. **36**, 168–259 (2010).
[9]S. Subramaniam and S. Pope, "Comparison of mixing model performance for nonpremixed turbulent reactive flow," Combust. Flame **117**, 732–754 (1999).
[10]B. Merci, D. Roekaerts, and B. Naud, "Study of the performance of three micromixing models in transported scalar PDF simulations of a piloted jet diffusion flame ('Delft Flame III')," Combust. Flame **144**, 476–493 (2006).
[11]F. Gao and E. E. O'Brien, "A large-eddy simulation scheme for turbulent reacting flows," Phys. Fluids **5**, 1282–1284 (1993).

[12]P. J. Colucci, F. A. Jaberi, P. Givi, and S. B. Pope, "Filtered density function for large eddy simulation of turbulent reacting flows," Phys. Fluids **10**, 499–515 (1998).
[13]A. Y. Klimenko, "Multicomponent diffusion of various admixtures in turbulent flow," Fluid Dyn. **25**, 327–334 (1990).
[14]A. Y. Klimenko and S. B. Pope, "The modeling of turbulent reactive flows based on multiple mapping conditioning," Phys. Fluids **15**, 1907–1925 (2003).
[15]M. J. Cleary and A. Y. Klimenko, "A detailed quantitative analysis of sparse-Lagrangian filtered density function simulations in constant and variable density reacting jet flows," Phys. Fluids **23**, 115102 (2011).
[16]R. W. Fox, P. J. Pritchard, and A. T. McDonald, *Introduction to Fluid Mechanics*, 6th ed. (Wiley, 2008).
[17]E. Madadi-Kandjani, R. O. Fox, and A. Passalacqua, "Application of the Fokker–Planck molecular mixing model to turbulent scalar mixing using moment methods," Phys. Fluids **29**, 065109 (2017).
[18]U. Piomelli, "Large eddy simulations in 2030 and beyond," Philos. Trans. R. Soc., A **372**, 20130320 (2014).
[19]L. Valiño, "A field Monte Carlo formulation for calculating the probability density function of a single scalar in a turbulent flow," Flow, Turbul. Combust. **60**, 157–172 (1998).
[20]O. Soulard and V. Sabel'nikov, "A new Eulerian Monte Carlo method for the joint velocity-scalar PDF equations in turbulent flows," in Proceedings of European Conference on Computational Fluid Dynamics (Netherlands, 2006).
[21]P. Langevin, "Sur la theorie du mouvement brownien," C. R. Acad. Sci. (Paris) **146**, 530–533 (1908).
[22]W. Kollmann, "A PDF closure for compressible turbulent chemically reacting flows," Technical Report No. NAG 3–836 (National Aeronautics and Space Administration - NASA, 1992).
[23]B. J. Delarue and S. B. Pope, "Application of PDF methods to compressible turbulent flows," Phys. Fluids **9**, 2704–2715 (1997).
[24]H. Möbus, P. Gerlinger, and D. Brüggemann, "Scalar and joint scalar-velocity-frequency Monte Carlo PDF simulation of supersonic combustion," Combust. Flame **132**, 3–24 (2003).
[25]P. Gerlinger, "Lagrangian transported MDF methods for compressible high speed flows," J. Comput. Phys. **339**, 68–95 (2017).
[26]M. B. Nik, P. Givi, C. K. Madnia, and S. B. Pope, "EPVS-FMDF for LES of high-speed turbulent flows," in Proceedings of 50th AIAA Aerospace Sciences Meeting Including the New Horizons Forum and Aerospace Exposition (Tennessee, 2012).
[27]L. Zhang, J. Liang, M. Sun, H. Wang, and Y. Yang, "An energy-consistency-preserving large eddy simulation-scalar filtered mass density function (LES-SFMDF) method for high-speed flows," Combust. Theory Modell. **22**, 1–37 (2018).
[28]L. Zhang, J. Liang, M. Sun, Y. Yang, H. Zhang, and X. Cai, "A conservative and consistent scalar filtered mass density function method for supersonic flows," Phys. Fluids **33**, 026101 (2021).
[29]Z. Huang, M. J. Cleary, and H. Zhang, "Application of the sparse-Lagrangian multiple mapping conditioning approach to a model supersonic combustor," Phys. Fluids **32**, 105120 (2020).
[30]M. B. Nik, S. L. Yilmaz, P. Givi, M. R. H. Sheikhi, and S. B. Pope, "Simulation of Sandia flame D using velocity-scalar filtered density function," AIAA J. **48**, 1513–1522 (2010).
[31]C. Gong, M. Jandi, X. Bai, J. Liang, and M. Sun, "Large eddy simulation of hydrogen combustion in supersonic flows using an Eulerian stochastic fields method," Int. J. Hydrogen Energy **42**, 1264–1275 (2017).
[32]D. Fredrich, W. Jones, and A. Marquis, "The stochastic fields method applied to a partially premixed swirl flame with wall heat transfer," Combust. Flame **205**, 446–456 (2019).
[33]T. Pant, U. Jain, and H. Wang, "Transported PDF modeling of compressible turbulent reactive flows by using the Eulerian Monte Carlo fields method," J. Comput. Phys. **425**, 109899 (2021).
[34]O. Soulard and V. Sabel'nikov, "Eulerian Monte Carlo method for solving joint velocity-scalar PDF: Numerical aspects and validation," Technical Report (The French Aerospace Lab ONERA, 2008).
[35]Y. P. Almeida and S. Navarro-Martinez, "Large eddy simulation of a supersonic lifted flame using the Eulerian stochastic fields method," Proc. Combust. Inst. **37**, 3693–3701 (2019).
[36]Y. P. Almeida and S. Navarro-Martinez, "Large eddy simulation of supersonic combustion using the Eulerian stochastic fields method," Flow, Turbul. Combust. **103**, 943–962 (2019).
[37]S. Pirozzoli, "Numerical methods for high-speed flows," Annu. Rev. Fluid Mech. **43**, 163–194 (2011).
[38]M. R. H. Sheikhi, T. G. Drozda, P. Givi, and S. B. Pope, "Velocity-scalar filtered density function for large eddy simulation of turbulent flows," Phys. Fluids **15**, 2321–2337 (2003).
[39]W. K. Bushe and H. Steiner, "Conditional moment closure for large eddy simulation of nonpremixed turbulent reacting flows," Phys. Fluids **11**, 1896–1906 (1999).
[40]C. B. Laney, *Computational Gasdynamics* (Cambridge University Press, Cambridge, UK, 1998).
[41]L. Y. M. Gicquel, P. Givi, F. A. Jaberi, and S. B. Pope, "Velocity filtered density function for large eddy simulation of turbulent flows," Phys. Fluids **14**, 1196–1213 (2002).
[42]A. Y. Klimenko, "The convergence of combustion models and compliance with the kolmogorov scaling of turbulence," Phys. Fluids **33**, 025112 (2021).
[43]A. Y. Klimenko and R. W. Bilger, "Conditional moment closure for turbulent combustion," Prog. Energy Combust. Sci. **25**, 595–687 (1999).
[44]H. Pitsch, "Large-eddy simulation of turbulent combustion," Annu. Rev. Fluid Mech. **38**, 453–482 (2006).
[45]J. Villermaux and J. C. Devillon, "Représentation de la coalescence et de la redispersion des domaines de ségrégations dans un fluide par un modèle d'interáction phénoménologique," in Proceedings of 2nd International Symposium on Chemical Reaction Engineering (Netherlands, 1972).
[46]D. C. Haworth and S. B. Pope, "A generalized Langevin model for turbulent flows," Phys. Fluids **29**, 387–405 (1986).
[47]S. B. Pope, "Computations of turbulent combustion: Progress and challenges," Symp. (Int.) Combust., [Proc.] **23**, 591–612 (1990).
[48]D. Azarnykh, S. Litvinov, and N. A. Adams, "Numerical methods for the weakly compressible Generalized Langevin Model in Eulerian reference frame," J. Comput. Phys. **314**, 93–106 (2016).
[49]T. Poinsot and S. Lele, "Boundary conditions for direct simulations of compressible viscous flows," J. Comput. Phys. **101**, 104–129 (1992).
[50]M. R. H. Sheikhi, P. Givi, and S. B. Pope, "Velocity-scalar filtered mass density function for large eddy simulation of turbulent reacting flows," Phys. Fluids **19**, 095106 (2007).
[51]E. Touber and N. Alferez, "Shock-induced energy conversion of entropy in non-ideal fluids," J. Fluid Mech. **864**, 807–847 (2019).
[52]C. K. W. Tam and J. C. Webb, "Dispersion-relation-preserving finite difference schemes for computational acoustics," J. Comput. Phys. **107**, 262–281 (1993).
[53]C. Bogey and C. Bailly, "A family of low dispersive and low dissipative explicit schemes for flow and noise computations," J. Comput. Phys. **194**, 194–214 (2004).
[54]E. F. Toro, M. Spruce, and W. Speares, "Restoration of the contact surface in the HLL-Riemann solver," Shock Waves **4**, 25–34 (1994).
[55]P. J. Martínez Ferrer, R. Buttay, G. Lehnasch, and A. Mura, "A detailed verification procedure for compressible reactive multicomponent Navier–Stokes solvers," Comput. Fluids **89**, 88–110 (2014).
[56]F. Guillois, N. Petrova, O. Soulard, R. Duclous, and V. Sabelnikov, "Stochastic partial differential equations as a tool for solving the joint velocity-scalar probability density function transport equation," in *Stochastic Processes: Fundamentals, Concepts and Applications* (Nova Science Publishers, 2017), pp. 107–147.
[57]J. Glimm, "Solutions in the large for nonlinear hyperbolic systems of equations," Commun. Pure Appl. Math. **18**, 697–715 (1965).
[58]E. Garnier, M. Mossi, P. Sagaut, P. Comte, and M. Deville, "On the use of shock-capturing schemes for large-eddy simulation," J. Comput. Phys. **153**, 273–311 (1999).
[59]E. Garnier, N. Adams, and P. Sagaut, *Large Eddy Simulation for Compressible Flows*, 1st ed. (Springer, Berlin, 2009).
[60]R. P. Fedkiw, B. Merriman, and S. Osher, "Numerical methods for thermally perfect gas flows with chemistry," J. Comput. Phys. **132**, 175–190 (1997).
[61]R. A. Yetter, F. L. Dryer, and H. Rabitz, "A comprehensive reaction mechanism for carbon monoxide/hydrogen/oxygen kinetics," Combust. Sci. Technol. **79**, 97–128 (1991).

[62]W. P. Jones, A. J. Marquis, and V. N. Prasad, "LES of a turbulent premixed swirl burner using Eulerian field method," Combust. Flame **159**, 3079–3095 (2012).
[63]L. Valiño, R. Mustata, and K. B. Letaief, "Consistent behavior of Eulerian Monte Carlo fields at low Reynolds numbers," Flow, Turbul. Combust. **96**, 503–512 (2016).
[64]H. Wang, "Fully consistent Eulerian Monte Carlo fields method for solving probability density function transport equations in turbulence modeling," Phys. Fluids **33**, 015118 (2021).
[65]W. P. Jones and S. Navarro-Martinez, "Large eddy simulation of autoignition with a subgrid probability density function method," Combust. Flame **150**, 170–187 (2007).